

## ON THE APPLICATION OF THE ONSAGER DFT THEORY TO TWO-DIMENSIONAL SYSTEM OF HARD NEEDLES

AGNIESZKA CHRZANOWSKA

Institute of Physics, Cracow University of Technology  
Podchorążych 1, 30-084 Kraków, Poland

(Received April 7, 2005; revised version received August 30, 2005)

We present a simple Onsager type density functional theory (DFT) of a two-dimensional system of hard needles and assume that it can be applied to describe intensive and short range properties of a real system which, on the other hand, on larger scales exhibits topological order. It is shown that the transition point of the isotropic-nematic transformation and the state equation obtained are almost the same as those predicted from the computer simulations [*Phys. Rev.* **A31**, 1776 (1985)] for small and undistorted system, which is never the case in liquid crystals, where these results are shifted in the density and require rescalings like, for instance, the Parson-Lee approach [*Phys. Rev.* **A19**, 1225 (1979); *J. Chem. Phys.* **87**, 4972 (1987); *J. Chem. Phys.* **89**, 7036 (1988).] Similar effect occurs for the chemical potential. Such behavior is attributed to the presence of negative values of higher virial coefficients, which may cancel the influence of the other positive coefficients in such a way that the second virial approximation gives accurate predictions. The above conclusion coincides with the Onsager idea that the second virial DFT theory for infinitely 3D hard particles is accurate. We notice that this coincidence comes from the fact that the 3D and 2D interaction models are governed by the same theoretical formulation. We also claim that the observed in the Monte Carlo simulation the disclinations unbinding process does not mean the change from the isotropic to the nematic phase (IN), as believed before, since the spontaneously drifting disclinations cannot be responsible for the changes of the system symmetry. The IN transition, as usual, is driven by the molecular interactions and the disclination unbinding must undergo then in the uniaxial phase. We also confirm that the chemical potential has a smooth character as a function of pressure, whereas it has an abrupt change in the slope at the point of transition while plotted *versus* density.

PACS numbers: 71.15.Mb, 64.70.Md, 61.30.-v

## 1. Introduction

Hard needles are the system which has been widely studied so far, both by the DFT approaches [2–5] and by the computer simulations [6–10]. A direct benefit of using this model is the easiness to understand the mechanisms that lead to different properties. Of special interest is the 2D system since it forms the liquid crystalline phase. A detailed analysis of its basic properties has been given in [9] on the basis of the Monte Carlo simulations. In this paper Frenkel *et al.* have presented the typical order parameter in the region, where the anisotropic phase has just set in, the equation of state, the chemical potential, the orientational correlations and the virial coefficients. The authors show that the higher than the second order virial coefficients are nonzero, but the fifth virial coefficient is negative. This feature may have its consequences as far as the Onsager theory [11] is concerned. As it will be shown, the Onsager type theory provides almost perfect predictions. This can be attributed to the fact that the higher than the second virial coefficients compensate each other in such a way that the second virial is strongly dominant. One can recall here a similar feature of the second virial DFT theories in 3D liquid crystals. Here, no matter what shape 3D molecules have, the longer they become the better results of the second virial DFT description are obtained.

In view of the above similarity it would be interesting to discuss in detail the correspondence of the DFT models in 3D and 2D cases. First of all one should mention that the only angle that is used in 2D description corresponds *directly* to the main (polar) angle of 3D description. Moreover, the interaction kernel, which corresponds to the excluded volume, for very elongated molecules is exactly the same in both cases, *i.e.* it is described by the function  $\sin(\phi_1 - \phi_2)$ . As a result the DFT equations for these two cases are almost the same. The differences in the properties arise *solely* from the Jacobian: in 2D case the Jacobian is simply 1, in 3D case it is the function  $\sin(\phi)$ . In 3D case, also the transition from the isotropic to the nematic phase is of the first order whereas in 2D case it is weakly second order.

The successful application of the second virial DFT descriptions for long molecules in 2D as in 3D cases undoubtedly corresponds to the fact that the interaction kernels are the same. If, for instance, the sum of the higher than second virial terms, say  $\sum_{3D}$ , is known from experience to be zero and can be written as

$$\sum_{3D} = \int_0^{\pi} h(\phi) \sin \phi d\phi = 0 \quad (1)$$

then this fact means that  $h(\phi)$  is antisymmetric with respect to the half of the integral interval,  $\phi = \pi/2$ , and, consequently also

$$\sum_{2D} = \int_0^{\pi} h(\phi) d\phi = 0. \quad (2)$$

Although the scope of the present paper is limited to small systems, for which we can use the assumption that the director is not distorted, we must mention that there is still another problem with 2D hard needles, which concerns the so-called topological order in large ensembles.

The topological order is the property of the system, in which the director is not fixed in space, but attains a spontaneous pattern of distorted branches with many disclinations. Such a picture is always obtained in the Monte Carlo simulations of 2D hard needles. In this case the statistical average, which is usually used to assess the order of the system (still called here the order parameter) depends on the number of the particles and when the system increases, its value systematically decreases (see [9]). However, on the short range scale and with respect to the local director the particles are very well ordered.

In the present paper we assume that these short range features can be reproduced by the Onsager theory of an undistorted system. This assumption gives very reasonable results if compared to the Monte Carlo data for a small system. It leads also to the conclusion that the possible Kosterlitz–Thouless (KT) unbinding transition [12] must undergo in the uniaxial phase. This unbinding transition denotes the situation, when disclinations drift apart from their companions, to which they were previously bound. What emerges from the paper [9]), the unbinding mechanism is the main reason for the symmetry change in the system (from anisotropic to isotropic), (similarly as in the case of the 2D solid melting [13, 14]). This belief contradicts the fact that the basic reason to change the symmetry of the liquid crystalline system are the molecular (or external fields) *interactions*. Contrary to the solid of 2D spherical particles, molecular interactions of 2D hard needles are anisotropic. In fact, this anisotropy is the strongest of all the possible hard bodies.

Despite the fact that the obtained in this paper DFT results of the thermodynamical properties refer to small systems, they are also relevant for large ensembles. According to the data presented in the state equation in Fig. 2, they give the major contributions to the total values. Moreover, they can be very useful to test the kinetic theories [15] and to calculate dynamical properties like relaxation times or diffusivities.

The paper is organized as follows. Section 2 presents the density functional theory. In Section 3 we perform the bifurcation analysis which

provides the bifurcation density at which the anisotropic phase starts to grow. Section 4 presents the results obtained for the pressure, order parameter, chemical potentials and heat capacities.

## 2. Density functional theory (second virial approximation)

The total energy of the nematic system  $F_{\text{tot}}$  can be given as a sum of the following terms:

$$F_{\text{tot}} = F_{\text{uni}} + F_{\text{elastic}} + F_{\text{exter}} + F_{\text{defects}}, \quad (3)$$

where  $F_{\text{uni}}$  describes the energy of the uniform (undistorted) system,  $F_{\text{elastic}}$  is the elastic energy of the Frank type which comes from the director deformations,  $F_{\text{exter}}$  corresponds to the energy contribution that originates from the interactions with external fields including surface interactions.  $F_{\text{defects}}$  corresponds to the energy of the possible defects.

The first term is the most fundamental for liquid crystals and the focus of the present paper is just an assessment of it for 2D hard needles on the basis of the DFT Onsager theory. This term can be directly compared to the simulation data if the simulated system is small enough to ensure that the director is undeformed. At the end of the paper we also provide a prognosis for the influence of the other two relevant terms,  $F_{\text{elastic}}$  and  $F_{\text{defects}}$  ( $F_{\text{exter}}$  in our case is zero).

For the system of  $N$  hard bodies, the free energy of undistorted system within the second virial approximation is given by

$$\begin{aligned} \frac{\beta F}{N} &= \frac{\beta F_0}{N} + \int f_1(\phi_1) [\log df_1(\phi_1) - 1 - \beta\mu] d\phi_1 \\ &+ \frac{1}{2}d \int V_{\text{excl}}(\phi_1, \phi_2) f_1(\phi_1) f_2(\phi_2) d\phi_1 d\phi_2. \end{aligned} \quad (4)$$

In the above the excluded volume of two confined to a plane needles follows a simple formula  $V_{\text{excl}} = L^2 |\sin(\phi_{12})|$ , where  $L$  is the length of the needle,  $d$  the density and  $\phi_{12}$  is the angle between the particles; the orientational distribution function,  $f(\phi) \equiv \text{ODF}$ , is normalized as  $\int_0^\pi f(\phi) d\phi = 1$  and  $F_0$  is a constant which can comprise as well the contribution from the de Broglie wavelength term as any shift determined by the zero choice of the energy level.

The equilibrium profile of the orientational distribution function  $f$  can be obtained using the minimum condition of the free energy (4). It leads to the self-consistency equation

$$\log f(\phi_1) = -\rho^* \int \sin(\phi_1 - \phi_2) f(\phi_2) d\phi_2 - \log d + \beta\mu, \quad (5)$$

where the reduced density is  $\rho^* = L^2 d$ .

We solve the equations (5) in a standard iterative way. However, the integration we use does not require any polynomial expansion neither to the integral kernel (here,  $V_{\text{excl}}$ ) nor to the functions ODF. In particular, we use the Gaussian quadrature scheme [16] with the total number of Gaussian points per interval equal to  $2 \times 16 = 32$  with a temporal storage of the ODF values at the last two iteration steps. As a result of the iterative procedure, we obtain then the solution as a set of the ODF values at the Gaussian points and the value of the chemical potential. Accuracy of the convergence is calculated as a cumulative sum of the differences between subsequent values of the ODF in the nearest two steps at all the Gaussian points and the program is stopped when this accuracy is less than  $10^{-8}$ . The obtained set of the values  $f(\phi_i)$  ( $\phi_i$  being the Gaussian point) is sufficient to calculate all the needed thermodynamical properties such as order parameters, pressure, free energy or characteristic heats. More detailed discussion about the above method to solve the DFT equations one can find also in [17], where it has been also adapted for the nematic in a slab geometry.

### 3. Bifurcation analysis

We will start our DFT investigations from finding the point of transition by the use of the bifurcation analysis. Bifurcation analysis is the simplest and the best tool by the use of which one can gain insight into the possibilities of the structural changes and the symmetries of the new phases. In the case of liquid crystals the recommended literature that provides the principles how to perform bifurcation analysis is given in the papers [18–22].

Following the line of notation from [18], let us rewrite the free energy as

$$\beta F = \langle f, \ln f \rangle + \frac{1}{2} \lambda \langle f, K[f] \rangle - \beta \mu, \quad (6)$$

where  $\langle \dots \rangle = \int \dots d\phi$ , and  $K[f] = \int K(\phi_1, \phi_2) f(\phi_2) d\phi_2$ .  $\lambda$  coincides with the reduced density  $\rho^*$ .

The minimization condition together with the appropriate normalization leads to the equation

$$f = \frac{\exp(-\lambda K[f])}{\langle 1, \exp(-\lambda K[f]) \rangle}. \quad (7)$$

In this form it is clearly visible that the kernel term  $K[f]$  plays the role of the self consistent “mean field”. Eq. (7) is the central object upon which the bifurcation analysis operates. To proceed one needs now explicit forms of the possible symmetry adapted functions and their relationship with the elements from Eq. (7). For 2D nematic, they take simply a form of  $\Delta^n = \cos n\phi$ , where  $n = 0, 2, 4, \dots$ .  $\Delta^n$ 's obey the normalization condition

$$\int \Delta^n \Delta^{n'} d\phi = \frac{1}{2} \pi \delta_{nn'}. \quad (8)$$

The interaction kernel can be cast as a series

$$K(\tilde{\phi}) = \sum_n \frac{2}{\pi} k_n \Delta^n(\tilde{\phi}). \quad (9)$$

For the Onsager particles interacting accordingly to the formula  $K(\tilde{\phi}) = \sin(\tilde{\phi})$ , some examples of the needed coefficients are  $k_2 = -\frac{2}{3}$ ,  $k_4 = -\frac{2}{15}$ ,  $k_6 = -\frac{2}{35}$ .

The next two formulas allow one to elaborate upon the interaction term

$$\int \Delta^n(\phi_1) \Delta^{n'}(\phi_2 - \phi_1) d\phi_1 = \frac{1}{2} \pi \Delta^n(\phi_2) \delta_{nn'}, \quad (10)$$

$$\begin{aligned} \int K(\phi_2 - \phi_1) \Delta^n(\phi_1) &= \sum_{n'} \int \frac{2}{\pi} k_{n'} \Delta^{n'}(\phi_2 - \phi_1) \Delta^n(\phi_1) d\phi_1 \\ &= \sum_n k_n \Delta^n(\phi_2). \end{aligned} \quad (11)$$

The bifurcation analysis in the first step looks for the solutions that branch off from the isotropic solution  $f_0 = 1/\pi$ . In the vicinity of the bifurcation point one can express the elements of Eq. (7) as expansions in the arbitrary small parameter  $\varepsilon$ :

$$\begin{aligned} f &= f_0 + \varepsilon f_1 + \varepsilon^2 f_2 \dots \\ \lambda &= \lambda_0 + \varepsilon \lambda_1 + \varepsilon^2 \lambda_2 \dots, \end{aligned} \quad (12)$$

where due to the normalization  $\langle 1, f_k \rangle = 0$  for  $k \geq 1$ .

Applying (12) to Eq. (7) and equating terms of equal order in  $\varepsilon$  one finds:

$$f_1 = -\frac{\lambda_0}{\pi} K[f_1], \quad (13)$$

$$\begin{aligned} f_2 &= -\frac{1}{\pi} \left[ \lambda_0 K[f_2] + \lambda_1 K[f_1] \right. \\ &\quad \left. - \frac{1}{2} \lambda_0^2 \left\{ K[f_1]^2 - \frac{1}{\pi} \langle 1, K[f_1]^2 \rangle \right\} \right]. \end{aligned} \quad (14)$$

The first equation (13) is commonly known as the bifurcation equation. Using now (9), (10) and (11) one obtains the condition

$$\lambda^{\text{bif}} = -\frac{\pi}{k_2}. \quad (15)$$

This gives the density of bifurcation as  $\rho^* = \pi/\frac{2}{3} = 4.7124$ , which is perfectly confirmed by the DFT results (see next section).

Now we attempt to justify that the phase transition predicted by the DFT theory is of the second order. Let  $k^*$  be an eigenvalue of the  $K[ ]$  with the corresponding eigenvector  $\chi$

$$K[\chi] = k^* \chi. \tag{16}$$

According to (13) any pair of  $[k^*, \chi]$  solves the bifurcation equation. The physical bifurcation is given then, as already shown above, by the absolutely largest eigenvalue of  $k^*$  (the smallest value of  $\lambda^{\text{bif}} = -\frac{\pi}{k^*}$ ), in our case it is  $k_2$  and the relevant eigenvector is simply  $\chi = \Delta^2$ .

The general solution is  $f_1 = S\chi$ , where the condition for the coefficient  $S$  must be assessed from the second equation (14). This can be done by taking the inner product of (14) with  $\chi$ :

$$\begin{aligned} \langle \chi, f_2 \rangle = & -\frac{1}{\pi} \left( \lambda_0 \langle \chi, K[f_2] \rangle + \lambda_1 \langle \chi, K[f_1] \rangle \right. \\ & \left. - \frac{1}{2} \lambda_0^2 \left\{ \langle \chi, K[f_1]^2 \rangle - \langle \chi, 1 \rangle \frac{1}{\pi} \langle 1, K[f_1]^2 \rangle \right\} \right). \end{aligned} \tag{17}$$

The last term is zero, since  $\langle \chi, 1 \rangle = 0$ . Let us note now:

$$\begin{aligned} \langle \chi, f_2 \rangle = & 1 \langle \chi, f_2 \rangle = -\frac{\lambda_0 k_2}{\pi} \langle \chi, f_2 \rangle, \\ -\frac{\lambda_0}{\pi} \langle k_2 \chi, f_2 \rangle = & -\frac{\lambda_0}{\pi} \langle K[\chi], f_2 \rangle = -\frac{\lambda_0}{\pi} \langle \chi, K[f_2] \rangle. \end{aligned} \tag{18}$$

Using this property one obtains from (17)

$$-\frac{1}{\pi} (\lambda_1 \langle \chi, K[f_1] \rangle - \frac{1}{2} \lambda_0^2 \langle \chi, K[f_1]^2 \rangle) = 0. \tag{19}$$

For  $f_1 = S\chi$  one derives next

$$\lambda_1 k_2 S \langle \chi, \chi \rangle - \frac{1}{2} \lambda_0^2 k_2^2 S^2 \langle \chi, \chi^2 \rangle = 0. \tag{20}$$

In contrast to the three-dimensional case, where the integral of three Legendre polynomials of the same order is nonzero, here  $\langle \chi, \chi^2 \rangle$  vanishes ( $\langle \Delta^2, \Delta^2 \Delta^2 \rangle = 0$ ). This property together with (20) leads to a trivial conclusion that  $\lambda_1 = 0$ . Vanishing of  $\lambda_1$ , according to [18], has a nontrivial consequence that the bifurcation is associated with the transition of higher order than the first order. In [18] a similar situation ( $\lambda_1 = 0$ ) has been shown for the isotropic-biaxial transition, which is known to be of the second order.

#### 4. Results

The DFT theory provides a sequence of properties which will be confronted against the computer simulation results, mainly from [9]. We will start our analysis from the properties of the orientational order. In Fig. 1 we present a profile of the order parameter obtained *versus* the density. It is calculated due to the definition  $S = \int \cos 2\phi f(\phi) d\phi$ , and presented as positive. The DFT results are given as white circles and the data obtained from the molecular dynamics [7] as grey squares. The black circles correspond to the Monte Carlo data of 200 needles from [9]. The order parameters above the transition point, *i.e.* in the nematic phase, obtained from the simulations and from the theory are more or less in coincidence. The parameters below the transition point, which we identify due to the DFT results as  $\rho^* = 4.7$ , are different. The simulations do not predict such a sharp rise in the order as the DFT theory does. It is not very clear what is the reason for such behavior. What is meaningful is the fact that the shape of the order parameter is a continuous curve that reminds of the letter ‘s’. Such a behavior indicates the second order type of the transition. However, since at the same time the rise of the order parameter is quite an abrupt one, it is similar also to the first order transition behavior. Such character of the isotropic-nematic transition is quite typical for 2D systems. It has been already mentioned in the case of the Onsager theory [2,9], also the 2D equivalent of the Maier–Saupe theory [23] predicts a continuous IN transition.

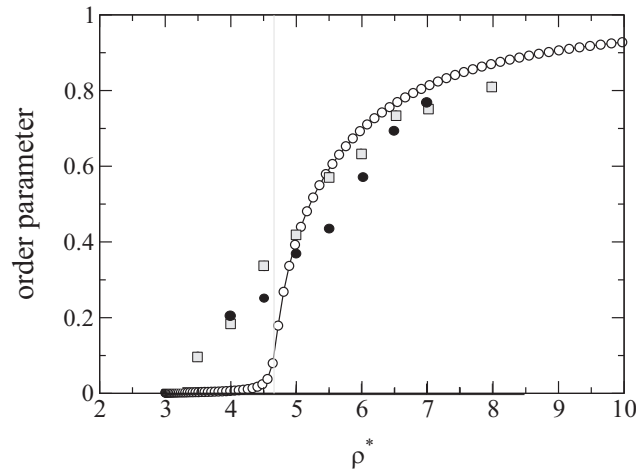


Fig. 1. Order parameter *versus* the density  $\rho^*$ . White circles are the data from the present paper theory and grey squares are from the molecular dynamics [7]. The black circles are the results of MC simulations of 200 needles from [9].

We should, however, mention again that the MC data used in this picture are only for 200 needles. Such a system is small enough to ensure that the director is not deformed. Also the molecular dynamics results in [7] have been obtained for undistorted system, which feature pertained within the whole simulation due to the assumed undeformed director in the initial configuration.

One should also realize that the picture of  $S$  will be much different if one considers MC data for larger systems. Then, the calculated values of the topological order parameter will form a curve similar in shape to the curve of 200 needles, but upon enlarging the system this curve will be systematically “shifted” toward higher densities (see Fig. 4 in the paper of Frenkel and Eppenga [9]) This feature is called as the finite size effect. Please note here that this effect comes mainly from the director spontaneous distortions (the  $S$  is an average calculated with respect to *the laboratory frame*).

The influence of the finite size effects on the order parameter seems to have been the reason in [9] of disregarding the bend in the state equation curve at about  $\rho^* = 4.7$  as the possible IN transition. The authors of [9] have paid attention, on the other hand, to the change that takes place at the density about  $\rho^* = 7.0$ . They have observed that the decay of the orientational correlations is algebraic at densities larger than  $\rho^* = 7.0$  and faster than algebraic at densities  $\rho^* < 7.0$ . Also, having developed a method to identify disclinations in the system, they could have observed that around  $\rho^* = 7.0$  there are still no free disclinations and below this density one can encounter already unbound pairs. This process has been then interpreted as the continuous transition of the Kosterlitz–Thouless type from the disordered to the algebraically ordered state. It seems now that the state below  $\rho^* = 7.0$  (in fact between  $\rho^* = 4.7$  and  $\rho^* = 7.0$ ) is not disordered but rather 2D uniaxial nematic.

In Fig. 2 we present the state equation  $\rho^*(P^*)$ , where the pressure is calculated from

$$\beta P = -\frac{\partial \beta F}{\partial V} = d + \frac{1}{2}d^2 \int V_{\text{excl}} f_1 f_2 d\phi_1 d\phi_2 \quad (21)$$

and  $P^* = PL^2$ .

The black dots represent the data from [9] and the solid line corresponds to the DFT predictions. The agreement is very good save for few points about the transition point where the DFT data underestimates the Monte Carlo simulations. In this picture and in what follows we will consequently use the MC data which are obtained for 200 particles. However, both thermodynamical variables here are of the intensive type and the MC data for larger system like 800 particles (crosses) do not differ much from the MC data for 200 needles. The difference can be well regarded as the statistical

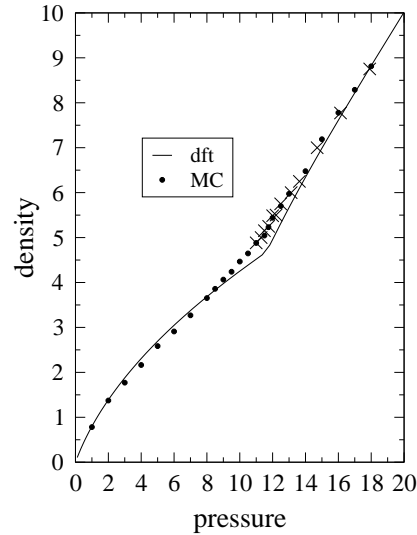


Fig. 2. The state equation,  $\rho^*(P^*)$ . The solid line is from the present DFT theory. The dots come from [9] for the system of 200 needles, for which system size the assumption of undistorted director still holds. The crosses are also from [9], but for the system of 800 needles. One observes that the crosses coincide with the results obtained for a small system. Because 800 needles already form certain distortions in the director these results can be regarded as a strong argument for the fact that the elastic energy and the energy of disclinations tend to cancel each other, see (3), for the systems with topological order.

error. What is important is a rather sudden change in the curve  $\rho^*(P^*)$ , which we attribute to the transition in the system structure. We call it the phase transition but one should remember that it is the feature which is driven by the presence of the local orientational order. Since this structural transition occurs at *each* point of the mesoscopic space, this supports our choice to call it the phase transition.

In [9], as already mentioned, the change of the slope at about  $P^* = 12$  has not been attributed to the isotropic-nematic transition. The paper [9] is focused on the disclination unbinding mechanism which is expected to have the transition point about  $\rho^* = 7.0$ . The authors have assumed that the unbinding of disclinations leads directly to the formation of the isotropic phase. Basing on the evidence of the so far presented data and on the next figures we now know that the point ( $P^* = 11.65$ ,  $\rho^* = 4.7$ ) is virtually the transition point from the isotropic phase to the ordered phase and the disclination unbinding transition takes place between two phases of the uniaxial order.

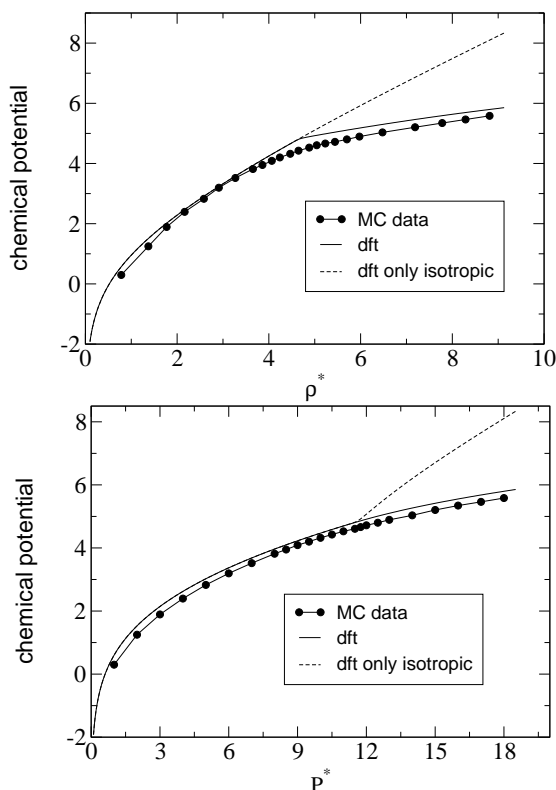


Fig. 3. (Upper panel): Chemical potential *versus*  $\rho^*$  and (lower panel): Chemical potential *versus*  $P^*$ . The dots come from [9], the solid line is from the present DFT theory and the dashed line is for the DFT results obtained for the purely isotropic phase.

For denser systems the pressure  $P^*$  approaches the value of  $2\rho^*$ . This limit can be obtained from (21) by the following reasoning. Multiplying (21) by  $L^2$  one has

$$pL^2 = \rho^* + \frac{1}{2}L^2d^2 \int L^2 \sin(\phi_1 - \phi_2)f_1f_2d\phi_1d\phi_2. \quad (22)$$

We assume that the ODF functions  $f_1$  and  $f_2$  are of the Dirac delta type and are peaked in such a way that the expression  $\langle \sin(\phi_1 - \phi_2) \rangle$  can be cast simply as  $x/L$ , where  $x$  stands for the available distance across the axis perpendicular to the needles, in which one can encounter two needles. Dividing our volume into boxes of the sides equal to  $x$  and to  $L$ , we may put forward a relation bounding the total particles number and the geometrical dimensions. Let us denote  $D$  as the size of the simulation box.

Particles are ordered along the  $Y$  direction, so the number of the possible rows is proportional to  $D/L$ . The number of the needles in a single row is determined by the size of the introduced  $x$  and follows:  $2D/x$ . Altogether one has  $N = 2D^2/Lx$ . The integral term in the formula (22) is then transformed into  $\frac{1}{2}L^4 \frac{N^2}{D^4} \frac{2D^2}{LN} \frac{1}{L} = d L^2 = \rho^*$  and  $P^* = pL^2 = 2\rho^*$ . This property is perfectly reconstructed by the DFT data (see the right upper corner of Fig. 2).

In Fig. 3 we present the chemical potential  $\mu - \pi$ , where  $\mu$  is calculated on the basis of the self consistency equations (5).  $\pi$  is regarded to come from  $F_0$ . Fig. 3 consists of two panels. The black circles are the data from the MC results and the curves are the DFT predictions. The comparison is again very satisfactory. The upper panel presents the dependence on the density whereas the lower one shows the dependence on the pressure. The pictures look similar, however, there is an important qualitative difference. The profile of  $\mu$  as dependent on the density  $\rho^*$  is bent at the transition toward the ordered phase, whereas the curve which shows  $\mu(P^*)$  is a smooth one and without any discontinuous change in the slope. The latter property has already attracted some comments in [9]. Since the type of the transition can be deduced not only from the behavior of the order, but also from other thermodynamical properties, Frenkel *et al.* concluded from the smoothness of the profile  $\mu(P^*)$  that the transition, if ever, cannot be the first order. This, of course, is true. It is interesting, however, to realize that many properties presented so far undergo abrupt changes, although continuous, whereas the chemical potential  $\mu$  as a function of  $P^*$  bears not even a shadow of a change in the slope and this fact seems to be a general feature.

In search of another piece of evidence about the transitions in hard needles, Frenkel *et al.* have evoked an example of the heat capacities. In general, there are two types of these quantities, the heat capacity at constant volume,  $C_V$ , and at constant pressure,  $C_P$ , (for convenience we skip here writing “\*”, since  $C_P = C_{P^*}$ ). The heat capacity at constant volume  $C_V$  is not very interesting, since it is equal to  $d/2$ , where  $d$  is the dimensionality of the system, so here  $C_V=1$ . In contrast,  $C_P$  is bound to the state equation  $\rho(P)$  through the relation

$$C_P = 1 + \frac{P^2}{\rho^2} \left[ \frac{\partial \rho}{\partial P} \right]_T. \quad (23)$$

This equation remains, of course, the same if we use the reduced values with “\*”.

In Fig. 4 we present a comparison of the  $C_P-C_V$  results that are obtained from the DFT theory and MC simulations. Again, the black circles are the data from the MC simulations and white circles are the DFT results.

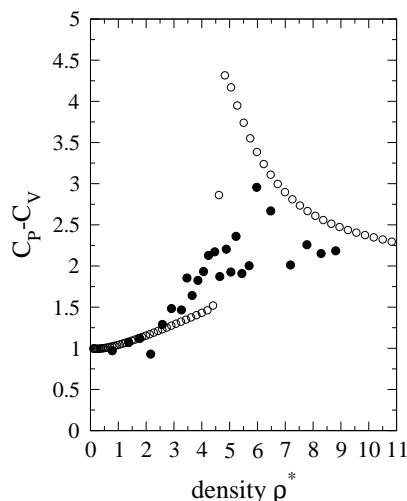


Fig. 4.  $C_P - C_V$  of a system of 2D hard needles as a function of  $\rho^*$ . Black circles are the data for the system of 200 needles from [9], white circles are the DFT results.

The Monte Carlo data have been discussed in [9] with much caution, since their character seemed to be a bit noisy. It has led the authors, however, to the idea that “ $C_P$  has a finite and rather broad peak around  $\rho^* = 5.5-6.0$ ” and that “the peak in  $C_P$  occurs at a higher density than the point where 2D Onsager model has its second-order phase transition ( $\rho_0^* = 4.71$ )”. Then, considering this profile of  $C_P$ , the behavior of  $\mu(P)$  and the state equation  $\rho(P)$ , Frenkel *et al.* drew a conclusion that “the thermodynamic properties of the hard needle fluid are not very sensitive to the onset of orientational order”. Now, looking at Fig. 4 all can agree that the noisy data fits quite well to the theoretical scenario and that the peak-like structure in the MC results occurs on the slope that arises just at the isotropic-nematic transition at the density  $\rho^* = 4.7$ . It makes an impression to be a peak structure due to the softening effect in the vicinity of the transition. The reason for such softening is not completely clear. One can observe it, however, also in the state equation (Fig. 2) and even more visibly in the order parameter itself (Fig. 1).

Since the possibility of the KT transition in the anisotropic phase is a novel idea we feel obliged to add more argument to back it up. Therefore for a moment we skip the assumption of small systems and take into consideration the ensemble with topological order, namely the system of 3200 needles. On the basis of the configurations obtained by us from the Monte Carlo simulations we have calculated the orientational correlation function  $g_2(r) = \langle \cos(2\phi - 2\phi_0) \rangle$  for different pressures. In a genuine nematic the long tail of  $g_2$

takes on the form of the parallel to the  $X$ -axis line, whose height corresponds to  $S^2$ . In the nematic with topological order it systematically declines. This case is observed in the Monte Carlo simulation, see Fig. 5. The thick line marks here the region where the DFT theory predicts the isotropic-nematic transition. The last curve (for  $P^* = 15$ ) is obtained for the vicinity, where, according to [9], the Kosterlitz–Thouless transition exists. There is a striking difference in the behavior of  $g_2$  below and above the pressure  $P^* = 11.65$  (the density  $\rho^* = 4.7$ ), where the DFT theory predicts transition. The phase above this density is characterized by the well observed growth and presence of the orientational order. By no means one can regard it as the same isotropic phase, for which the long tails of  $g_2$  remain almost on the zero level. The change of the  $g_2$  character below and above the DFT transition point is even more visible in Fig. 6, where we present the behavior of  $g_2$  on the more accurate logarithmic scale. We hope that these two pictures are a sufficient argument to support our idea that the KT transition ( $\rho^* = 7.0$ ) takes place *within* the anisotropic phase.

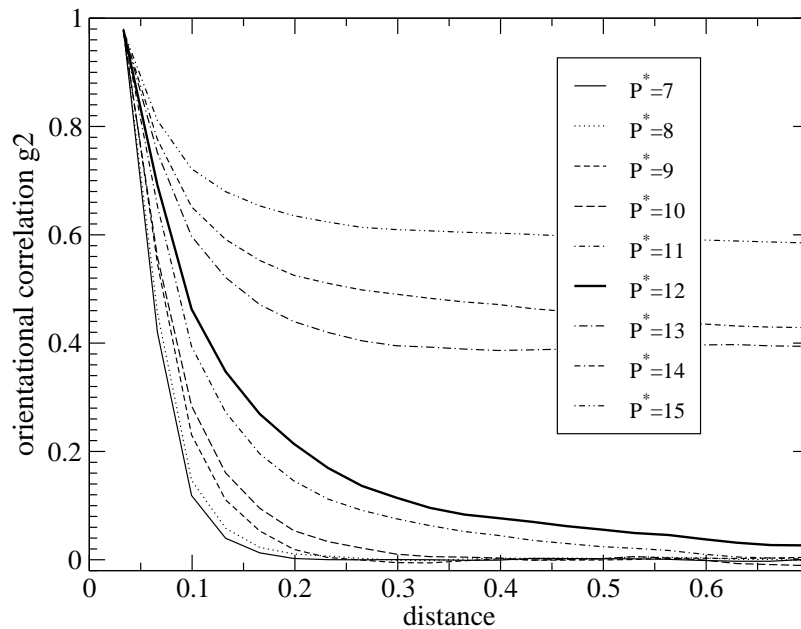


Fig. 5. The orientational correlation  $g_2$  obtained for different pressures from the Monte Carlo simulations performed on the system of 3200 needles. The thick line (for  $P^* = 12$ ) lies in the vicinity of the transition point predicted by the Onsager theory (for  $P^* = 11.65$ ). There is a striking difference of the behavior of  $g_2$  in the isotropic phase, below  $P^* = 11.65$ , and above this point.

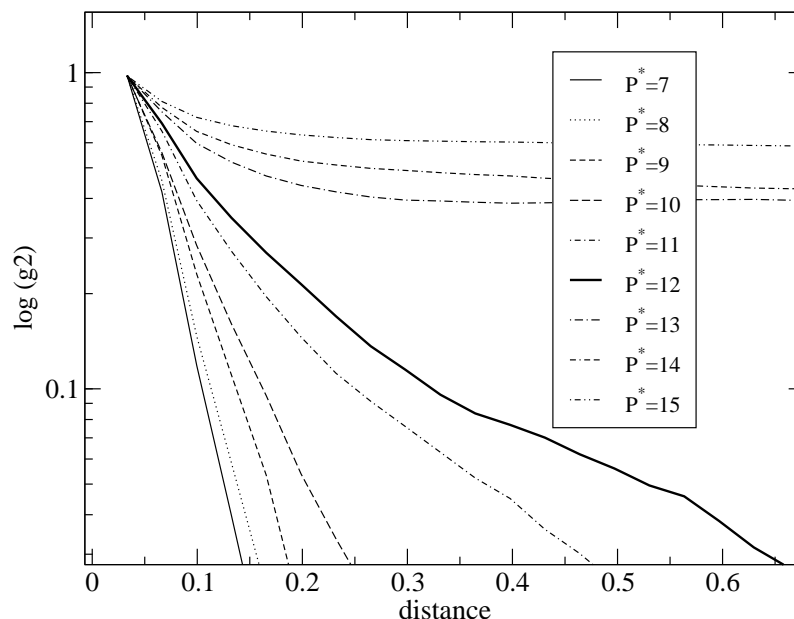


Fig. 6. The same as in Fig. 5, but on the more accurate logarithmic scale.

We thank Daan Frenkel and Lech Longa for reading the manuscript and their comments. The calculations have been made under the Cyfronet grant MNI/SG2800/PK/2004.

#### REFERENCES

- [1] J.D. Parsons, *Phys. Rev.* **A19**, 1225 (1979); S.-D. Lee, *J. Chem. Phys.* **87**, 4972 (1987); S.-D. Lee, *J. Chem. Phys.* **89**, 7036 (1988).
- [2] R.F. Kayser, H.J. Raveche, *Phys. Rev.* **A17**, 2067 (1978).
- [3] A. Poniewierski, *Phys. Rev.* **E47**, 3396 (1993).
- [4] A. Poniewierski, R. Holyst, *Phys. Rev.* **A38**, 3721 (1988).
- [5] Y. Mao, P. Bladon, H.N.W. Lekkerkerker, M.E. Cates, *Mol. Phys.* **92**, 151 (1997).
- [6] A. Chrzanowska, *J. Chem. Phys.* **120**, 2857 (2004).
- [7] A. Chrzanowska, H. Ehrentraut, *Phys. Rev.* **E66**, 012201 (2002).
- [8] D. Frenkel, J.F. Maguire, *Mol. Phys.* **49**, 503 (1983).
- [9] D. Frenkel, R. Eppenga, *Phys. Rev.* **A31**, 1776 (1985).
- [10] M.A. Bates, D. Frenkel, *J. Chem. Phys.* **112**, 10034 (2000).
- [11] L. Onsager, *Ann. N.Y. Acad. Sci.* **51**, 627 (1949).

- [12] J.M. Kosterlitz, D. Thouless, *J. Phys. C* **6**, 1181 (1973).
- [13] D.R. Nelson, B.I. Halperin, *Phys. Rev.* **B19**, 2457 (1979).
- [14] A.P. Young, *Phys. Rev.* **B19**, 1855 (1979).
- [15] Here, we mean the application of the DFT theory results to the Enskog theory of the velocity autocorrelations. In preparation.
- [16] W.H. Press, S.A. Teukolsky, W.T. Vetterling, B.P. Flannery, *Numerical Recipes in C: The Art of Scientific Computing*, Cambridge University Press, 2nd edition, January 1993.
- [17] A. Chrzanowska, *J. Comput. Phys.* **191**, 265 (2003).
- [18] B. Mulder, *Phys. Rev.* **A39**, 360 (1989).
- [19] L. Longa, *J. Chem. Phys.* **85**, 2974 (1986).
- [20] L. Longa, *Z. Phys.* **B85**, 357 (1986).
- [21] L. Longa, *Liq. Cryst.* **5**, 443 (1989).
- [22] A. Chrzanowska, *Phys. Rev.* **E58**, 3229 (1998).
- [23] J.Y. Denham, G.R. Luckhurst, C. Zannoni, *Mol. Cryst. Liq. Cryst.* **60**, 185 (1980).